Microscopic Description of Deeply Virtual Compton Scattering off Spin-0 Nuclei.

S. Liuti[1,*] and S. K. Taneja[1,†]

[1] *University of Virginia, Charlottesville, Virginia 22901, USA.*

We evaluate within a microscopic calculation the contributions of both coherent and incoherent deeply virtual Compton scattering from a spin-0 nucleus. The coherent contribution is obtained when the target nucleus recoils as a whole, whereas for incoherent scattering break-up configurations for the final nucleus into a an outgoing nucleon and an $A-1$ system are considered. The two processes encode different characteristics of generalized parton distributions.

PACS numbers: 13.60.-r, 12.38.-t, 24.85.+p

arXiv:hep-ph/0505123v1 13 May 2005

Recent theoretical and experimental developments have identified a new frontier for studies of the quark and gluon content of hadronic systems in a class of high energy exclusive processes. Their prototype is Deeply Virtual Compton Scattering (DVCS) [1]. DVCS provides observables that are most straightforwardly related to Generalized Parton Distributions (GPDs), the new theoretical tools introduced in [2, 3, 4] to describe in a partonic language the orbital angular momentum carried by the nucleon's constituents. GPDs were found more recently to describe also partonic structure in the transverse direction with respect to the large longitudinal momentum in the reaction. They are, in fact, the Fourier transforms of the so-called Impact Parameter dependent Parton Distributions Functions (IPPDFs) [5].

DVCS on a proton target, $ep \to e'p\gamma$, allows one to unravel in principle four GPDs: the unpolarized quark distributions, $H^q(X,\zeta,t)$, and $E^q(X,\zeta,t)$, and the polarized ones, $\widetilde{H}^q(X,\zeta,t)$, and $\widetilde{E}^q(X,\zeta,t)$. The kinematical variables are: $P'=P-\Delta$, $k'=k-\Delta$, the final nucleon's and quark's momenta, respectively; q, the virtual photon momentum, and $q'=q+\Delta$, the outgoing photon momentum. Furthermore: $-\Delta^2=t$, $X=k^+/P^+$, $\zeta=\Delta^+/P^+$ (Fig.1). [1] GPDs, or the correlation functions in the diagram, correspond to "hybrid" distributions in that they encode properties of both Parton Distributions Functions (PDFs) from inclusive Deep Inelastic Scattering (DIS), and of the proton form factors. In the (forward) limit: $t,\zeta \to 0$, $H^q(X,\zeta,t)=q(x)$, and $\widetilde{H}^q(X,\zeta,t)=\Delta q(x)$, the PDFs for polarized and unpolarized DIS, respectively. At the same time, GPDs first moments in X are given by the proton Dirac and Pauli form factors in the unpolarized case, and by the axial-vector and pseudo-scalar form factors in polarized scattering.

The first DVCS measurements were performed at HERA [6, 7, 8] and at CLAS [9]. Because of the presence of the Bethe-Heitler (BH) process producing the same $ep\gamma$ final state and dominating the cross sections at currently available kinematics, GPDs can be obtained only through the interference term between the DVCS and BH processes. In Born approximation, one writes:

$$T^2 = |T_{DVCS}|^2 + |T_{BH}|^2 + \mathcal{I} \tag{1}$$

Where $\mathcal{I}$, the interference term, is given by,

$$\mathcal{I} = [T_{DVCS}T^*_{BH} + T^*_{DVCS}T_{BH}] \tag{2}$$

At leading order in the four-momentum transfer $Q \equiv (-q^2)^{1/2}$ (twist-two), the contribution of $\mathcal{I}$ to the cross section is expressed as a finite sum of Fourier terms [10]:

$$\mathcal{I} \;=\; \mathcal{K}\left[c^{\mathcal{I}}_o + \sum_{n=1}^{3}\left(c^{\mathcal{I}}_n\cos(n\phi) + s^{\mathcal{I}}_n\sin(n\phi)\right)\right], \tag{3}$$

where $\mathcal{K}$ is a kinematical factor, and ϕ is the azimuthal angle between the lepton plane and the scattered hadron plane. The dominant harmonics are for $n=1$, the higher order ones being suppressed by α_S [10]. Several asymmetries (beam spin, A_{LU}, charge, A_C, target spin A_{UL}, etc...) have been identified, through which one can access $\mathcal{I}$, and probe different GPDs, or components of GPDs (see *e.g.* [1]).

GPDs were recently also measured through leptoproduction of a photon off nuclear targets, $eA \to e'\gamma A$ [11]. The study of nuclear targets is particularly important as they provide a laboratory where additional information can be obtained on these elusive observables. Exploratory studies using GPDs were performed both on the phenomenon of Color Transparency [12, 13, 14], *i.e.* on the rate of survival of small size hadronic configurations as the quasi-elastically struck nucleons scatter through the nuclear medium, and on the "generalized" EMC effect *i.e.* on the modifications of the nuclear GPDs with respect to the free nucleon ones, normalized to their respective form factors [15, 16, 17]. In [17], in particular, it was shown that the role of partonic transverse degrees of freedom, accounted for by a careful consideration of nucleon off-shellness, is enhanced in the generalized EMC effect, with respect to the forward case. In addition, a number of interesting relationships were found by studying Mellin moments in nuclei: the A-dependence for the D-term of GPDs was estimated within a microscopic approach, and compared with the calculation of [18] using

*sl4y@virginia.edu

†skt6c@virginia.edu

[1] We use the notation: $p^{\pm} = \frac{1}{\sqrt{2}}(p_o \pm p_3)$, with $(pk) = p^+k^- + p^-k^+ - p_\perp \cdot k_\perp$.

a liquid drop model, and finally, a connection was made with the widely used approaches that relate the modifications of "partonic" parameters such as the string tension, or the confinement radius, to density dependent effects in the nuclear medium (see *e.g.* [19] and references therein). These results designate nuclear GPDs as a potentially important new tool to investigate nuclear hadronization and related phenomena, which are vital for interpreting current and future data from RHIC, LHC, HERMES, and Jefferson Lab.

The qualitatively new insight offered by nuclear GPDs calls both for a more detailed study of the feasibility of experiments, and for more detailed studies aimed at establishing a better connection between GPDs and observables. In this paper we concentrate on spin-0 nuclei, with the aim of disentangling those nuclear effects that can be reconducted to the forward EMC effect [20]. Studies of nuclei with different spin, such as the deuteron, are at variance with ours since, due the more complex spin structure, they involve completely new functions with respect to the forward case therefore making it less linear to investigate the nature of nuclear medium modifications. [2]

The structure of the cross section for DVCS off a spin-0 nucleus involves the matrix elements in Eq.(1), similarly to proton case, with few important changes that we describe below. In particular, the nuclear GPDs can be extracted from similar types of asymmetries as for the proton case discussed above. Here we present a calculation for the nuclear beam spin asymmetry, $A_{LU}^{(A)}(\phi)$. $A_{LU}^{(A)}$ has been recently measured using D, Ne, and Kr targets at HERA [11]. Furthermore, a number of experiments are currently planned at HERA [11] and Jefferson Lab [21]. It is therefore now mandatory to provide *quantitative* evaluations of the generalized parton distributions entering the definition of $A_{LU}^{(A)}$. This reads:

$$A_{LU}^{(A)} = \frac{d\sigma^{\uparrow} - d\sigma^{\downarrow}}{d\sigma^{\uparrow} + d\sigma^{\downarrow}} \approx \frac{s_1^{\mathcal{I}}}{c_o^{BH}} \sin\phi. \tag{4}$$

The full expressions for the coefficients $s_1^{\mathcal{I}}$ and c_o^{BH} can be found in Appendix B of Ref.[10] and will not be repeated here. One can extract from such expressions the dominant contribution to Eq.(4) for a spin-0 nucleus, namely:

$$s_1^{\mathcal{I}} \propto \Im\mathrm{m}\, \mathcal{H}_A\, F_A(t),$$

$$c_o^{BH} \propto [F_A(t)]^2,$$

$F_A(t)$ being the nuclear form factor. By adopting the notation of [17] which extends the variables and functions defined in [22] to the nuclear case, one can write:

$$\Im\mathrm{m}\, \mathcal{H}_A(X,\zeta,t) = -\pi \sum_q e_q^2 \left[H_A^q(\zeta,\zeta,t) + H_A^{\bar{q}}(\zeta,\zeta,t)\right], \tag{5}$$

where we have introduced the nuclear GPDs, $H_A^{q(\bar{q})}$.

However, for a nuclear target two distinct classes of final states can occur, both in DVCS and BH: *i)* the scattering can happen *coherently*, that is the target nucleus recoils as a whole while emitting a photon with momentum q' (Figs.1a and 1c); *ii)* the nucleus undergoes breakup – or *incoherent* scattering – the final photon being emitted from a quasi-elastically scattered nucleon (Figs.1b and 1d).

The contribution from coherent scattering (Figs.1a, 1c) is given by a *product* of amplitudes:

$$\mathcal{I}_{coh}(\zeta,t) = \mathcal{K}\, \mathcal{F}_{DVCS}^A(\zeta,t) F_{BH}^A(t), \tag{6}$$

with:

$$\mathcal{F}_{DVCS}^A(\zeta,t) = \int \frac{d^2P_\perp dY}{2(2\pi)^3} \mathcal{N}\, \rho^A(Y,P^2;\zeta,t) \times \mathcal{F}_{DVCS}^N\left(\frac{\zeta}{Y},P^2;\frac{\zeta}{Y},t\right), \tag{7a}$$

$$F_{BH}^A(t) = \int \frac{d^2P_\perp dY}{2(2\pi)^3} \mathcal{N}\, \rho^A(Y,P^2;\zeta,t) F_1^N(t), \tag{7b}$$

where the nucleon (N) amplitude, in the small ζ approximation, *i.e.* by disregarding $E^{q(\bar{q})}$, is given by:

$$\mathcal{F}_{DVCS}^N \approx \sqrt{1-\zeta} \sum_q e_q^2 \left[H^q(\zeta,\zeta,t) + H^{\bar{q}}(\zeta,\zeta,t)\right] \tag{8}$$

Eq.(7a) was derived in [17]. In the forward limit – $\zeta, t \to 0$ – it yields the Deep Inelastic Scattering (DIS) nuclear structure function. Its ratio to the proton amplitude allows one to study the "generalized" EMC effect. Eq.(7b) is by definition the nuclear form factor, namely $F^A(t) \equiv F_{BH}^A(t)$.

The kinematical variables in Eqs.(6-8) are defined as: $Y = P^+/(P_A^+/A)$, the Light Cone (LC) nuclear momentum fraction taken by the struck nucleon (per nucleon), $X/Y = k^+/P^+$, the LC momentum fraction taken by the struck quark, P^2, the nucleon virtuality, $\zeta \equiv \Delta^+/(P_A^+/A)$, and $\zeta/Y = \Delta^+/P^+$, the skewedness with respect to the nucleon. Furthermore, $\mathcal{N} = (Y - \zeta/2)(\sqrt{Y(Y-\zeta)})$, is a normalization factor whose form derives from the normalization of the nucleon spinors in the off-forward case [17]; $\rho^A(Y,P^2;\zeta,t)$ is the off-forward LC nuclear spectral function [17], accounting for all configurations of the final nuclear system (see [23] and references therein for definitions in the forward case). When the dependence on P^2 is disregarded, ρ^A can be written within a non-relativistic approximation as:

$$\rho_A^{NR}(Y,\zeta,t) = 2\pi M \int_{P_{min}(Y,\overline{E})}^{\infty} dP P \Phi_A(P) \Phi_A^*(P').$$

[2] Our calculations however can be applied straightforwardly to the deuteron $\mathcal{H}_1$ function, or to channels where only one of the deuteron functions dominates.

where P, and P' are the incoming and outgoing nucleons three-momenta, Φ_A is the nuclear wave functions in momentum space; $\overline{E}$, is the average separation energy characterizing the final nuclear system. Eq.(7a) then becomes a longitudinal convolution in the variable Y.

For incoherent scattering, we consider the matrix elements for the nuclear DVCS and BH processes, respectively, with a break-up of the final nucleus. These can be read from Fig.1b and Fig.1d, respectively, as:

$$M^A_{inc-DVCS} = \left[\overline{U}(P',S')\overline{\Gamma}(k',P)\frac{(\not{k}'+m)}{k'^2-m^2}\frac{(\not{k}+m)}{k^2-m^2}\Gamma(k,P)U(P,S)\right]\left[\frac{(\not{P}+M)}{P^2-M^2}\Gamma_A(P,P_{A-1})U_{A-1}(P_A,S)\right], \quad (9)$$

$$M^A_{inc-BH^*} = \frac{1}{2P^+}\left[\overline{U}(P',S')[\gamma^+F_1(t)+\frac{i\sigma^{+\nu}\Delta_\nu}{2M}F_2(t)]U(P,S)\right]\left[\overline{U}_{A-1}(P_A,S)\overline{\Gamma}_A(P,P_{A-1})\frac{(\not{P}+M)}{P^2-M^2}\right] \quad (10)$$

where, similarly to Ref.[17], the nucleon vertex is described by a quark-diquark model, Γ being the vertex function, $U(P,S)$, $U(P',S')$ the nucleon spinors; Γ_A is the nuclear vertex function, and U_{A-1} describes the $A-1$ system.

For incoherent scattering, the interference term contributing to Eq.(1) is therefore given in the small ζ limit by a *convolution*:

$$\begin{aligned}\mathcal{I}_{inc}(\zeta,t) &= \mathcal{K}\int\frac{d^2P_\perp dY}{2(2\pi)^3}\mathcal{N}\,\rho_0^A(Y,P^2)\\ &\times\ \mathcal{F}^N_{DVCS}\left(\frac{X}{Y},P^2;\frac{\zeta}{Y},t\right)F_1^N(t)\\ &\equiv\ \mathcal{F}^A_{DVCS,0}(\zeta,t)F_1^N(t),\end{aligned} \quad (11)$$

where, within the nuclear impulse approximation illustrated in Fig.1, no momentum is transfered to the nuclear vertex. Therefore, at variance with coherent scattering, only the forward LC nuclear spectral function, $\rho_0^A(Y,P^2)=\rho^A(Y,P^2;\zeta=0,t=0)$, enters the calculation.

Next, we consider the numerical impact of both the coherent and incoherent processes on the asymmetry, $A_{LU}^{(A)}$. By including the contributions of both Eq.(6), nd Eq.(11) in Eq.(4), one has:

$$\begin{aligned}A_{LU}^{(A)} &\propto \frac{Z^2\left[\mathcal{F}^A_{DVCS}(\zeta,t)F_A(t)\right]+Z\left[\mathcal{F}^A_{DVCS,0}(\zeta,t)F_1(t)\right]}{Z^2F_A^2(t)+ZF_1^2(t)}\\ &\times\ \sin\phi.\end{aligned} \quad (12)$$

where Z is the number of protons, $F_1(t)$ is the proton form factor; in Eq.(12) the neutron contributions, H_n, F_1^n, were disregarded. Furthermore, similarly to Ref.[17], we consider only valence quarks contributions. These are expected to dominate the asymmetries at the kinematics of [6, 9, 11], namely at low Q^2 and intermediate values of Bjorken x, x_{Bj}. All form factors in Eq.(12) are normalized to unity and, correspondingly, $H_d=(1/2)H_u$.

By setting:

$$\mathcal{I}^A_{coh}=\left[\mathcal{F}^A_{DVCS}(\zeta,t)F_A(t)\right],\ \ \mathcal{I}^A_{incoh}=\left[\mathcal{F}^A_{DVCS,0}(\zeta,t)F_1(t)\right],$$

the ratio of the nuclear to proton asymmetry at leading order can be written as:

$$R_{LU}^{(A)}(\zeta,t)=\frac{Z^2\mathcal{I}^A_{coh}+Z\mathcal{I}^A_{incoh}}{\mathcal{F}^p_{DVCS}(\zeta,t)F_1(t)}\times\frac{F_1^2(t)}{Z^2F_A^2(t)+ZF_1^2(t)} \quad (13)$$

Notice that in the absence of incoherent scattering, and in the small ζ limit, $R_{LU}^{(A)}$ becomes the off-forward EMC effect ratio calculated in [17]:

$$R_A(\zeta,t)=\frac{H^A(\zeta,t)/F^A(t)}{H^N(\zeta,t)/F^N(t)}. \quad (14)$$

The behavior of $R_{LU}^{(A)}(\zeta,t)$ is shown in Figs.2 and 3. In Fig.2 we plot the following quantities: *i)* $R_{LU}^{(A)}(\zeta,t)$, as given in Eq.(13); *ii)* the DVCS coherent contribution to the ratio:

$$R_{LU}^{coh\,(A)}(\zeta,t)=\frac{Z^2\mathcal{I}^A_{coh}}{\mathcal{F}^p_{DVCS}(\zeta,t)F_1(t)}\times\frac{F_1^2(t)}{Z^2F_A^2(t)+ZF_1^2(t)} \quad (15)$$

iii) the DVCS incoherent contribution to the ratio:

$$R_{LU}^{incoh\,(A)}(\zeta,t)=\frac{Z\mathcal{I}^A_{incoh}}{\mathcal{F}^p_{DVCS}(\zeta,t)F_1(t)}\times\frac{F_1^2(t)}{Z^2F_A^2(t)+ZF_1^2(t)} \quad (16)$$

All calculations were performed for the ^4He nucleus, as

a prototype of spin-0 complex nuclei [3] using the microscopic nuclear model described in Ref.[17]. Results were summarized in two panels, Fig.2a and Fig.2b, in order to better illustrate the role played by particles' off-shellness within our microscopic nuclear model. As explained in detail in Ref.[17] the account of nucleons' off-shellness translates into a different, A-dependent relation between the struck quark's transverse degrees of freedom in a proton and in a nucleus, respectively, which is emphasized in off-forward observables such as GPDs. Off-shell effects are in fact quite noticeable, as seen by comparing Fig.2a, where they were disregarded, and Fig.2b. Moreover, both panels show Eqs.(13,15,16) at $x_{Bj} = 0.1$ and in the range: $0 < t < 0.5$ GeV^2. Clearly, incoherent DVCS dominates the asymmetries at $t \gtrsim 0.05$ GeV^2, that is in the range of recent HERMES data [11]. Also, our microscopic approach predicts an enhancement which is consistent with the HERMES data. Fig.3 shows the "coherent" and "incoherent" contributions separately, obtained by including also separately the contributions in the BH term in Eqs.(15) and (16). These contributions could be observed by detecting one of the outgoing nuclear constituents, as planned in future experiments [11]. Our calculation points out that the nuclear effects are expected to similar, in both cases, since they originate from similar modifications of the deep inelastic structure of the nucleus, encoded in our model in Eq.(7a) for coherent, and Eq.(11) for incoherent scattering (the two equations differ only in the nuclear t dependence, that does not affect the deep inelastic structure).

In conclusion, we presented for the first time quantitative evaluations of the coherent and incoherent contributions to the ratio of the nuclear beam spin asymmetry over the proton one. Although incoherent scattering dominates current experiments, interesting information can still be extracted relating the off-forward EMC effect to the previously measured, and still for many aspect puzzling, forward EMC effect. The difference between the coherent and incoherent cases can in fact be traced to the replacement of the off-forward LC nuclear spectral function with the forward one in the coherent case. This affects the t dependence of the nuclear wave functions, and has little impact on the modifications of the deep inelastic structure of a bound nucleon.

[1] M. Diehl, Phys. Rept. **388**, 41 (2003).
[2] D. Muller, D. Robaschik, B. Geyer, F. M. Dittes and J. Horejsi, Fortsch. Phys. **42**, 101 (1994)
[3] X. D. Ji, Phys. Rev. D **55**, 7114 (1997)
[4] A. V. Radyushkin, Phys. Rev. D **56**, 5524 (1997)
[5] M. Burkardt, Int. J. Mod. Phys. A **18**, 173 (2003); *ibid* Phys. Rev. D **62**, 071503 (2000) [Erratum-ibid. D **66**, 119903 (2002)].
[6] A. Airapetian *et al.* [HERMES Collaboration], Phys. Rev. Lett. **87**, 182001 (2001).
[7] C. Adloff *et al.* [H1 Collaboration], Phys. Lett. B **517**, 47 (2001)
[8] S. Chekanov *et al.* [ZEUS Collaboration], Phys. Lett. B **573**, 46 (2003)
[9] S. Stepanyan *et al.* [CLAS Collaboration], Phys. Rev. Lett. **87**, 182002 (2001).
[10] A. Kirchner and D. Muller, Eur. Phys. J. C **32**, 347 (2003).
[11] F. Ellinghaus, R. Shanidze, and J. Volmer, hep-ex/0212019; D. Hasch, *private communication.*
[12] J. P. Ralston and B. Pire, Phys. Rev. D **66**, 111501 (2002).
[13] M. Burkardt and G. A. Miller, arXiv:hep-ph/0312190.
[14] S. Liuti and S.K. Taneja, Phys. Rev. D **70**, 074019 (2004).
[15] V. Guzey and M. Strikman, Phys. Rev. **C 68**, 015204 (2003).
[16] S. Scopetta, Phys. Rev. C **70**, 015205 (2004).
[17] S. Liuti and S.K. Taneja, hep-ph/0504027.
[18] M. V. Polyakov, Phys. Lett. B **555**, 57 (2003).
[19] A. Accardi, D. Grunewald, V. Muccifora and H. J. Pirner, arXiv:hep-ph/0502072.
[20] J. J. Aubert *et al.* [European Muon Collaboration], Phys. Lett. B **123**, 275 (1983).
[21] Jefferson Lab Proposal, E-03-106, Spokeperson: F. Sabati/'e.
[22] K. J. Golec-Biernat and A. D. Martin, Phys. Rev. D **59**, 014029 (1999).
[23] C. Ciofi Degli Atti and S. Liuti, Phys. Lett. B **225** (1989) 215; *ibid* Phys. Rev. C **41**, 1100 (1990).

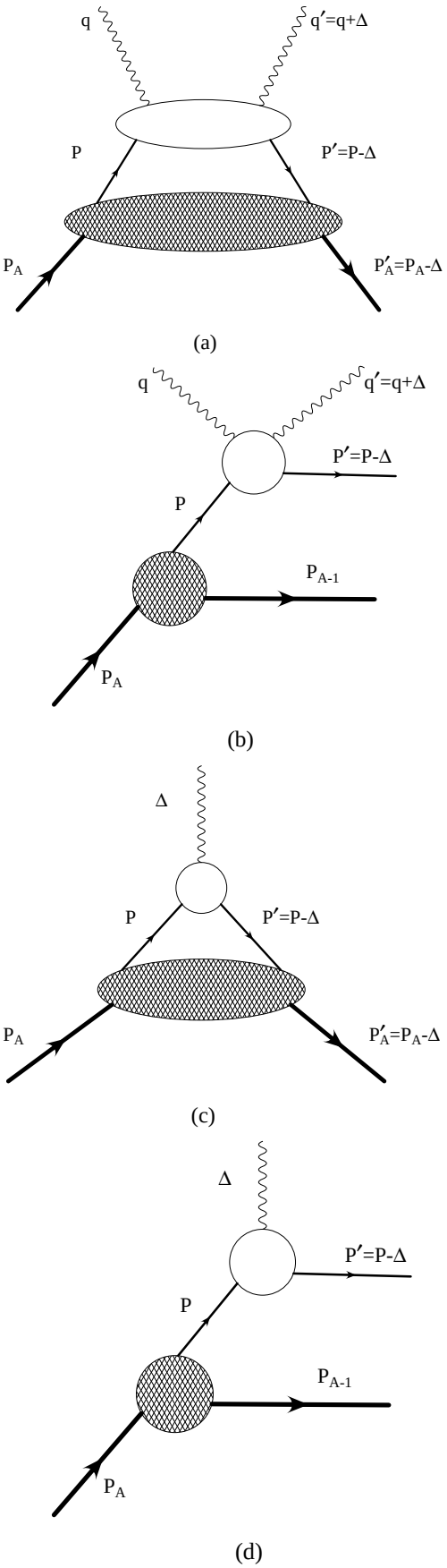

FIG. 1: Amplitudes for DVCS and BH processes from a nuclear target at leading order in Q. **(a)** DVCS, coeherent process; **(b)** DVCS, incoherent process; **(c)** BH, coeherent process; **(d)** BH, incoherent process.

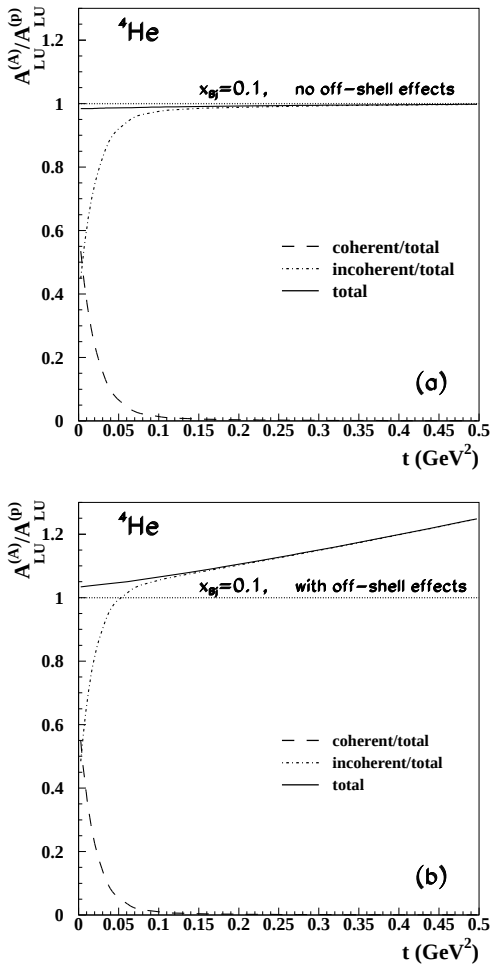

FIG. 2: Ratios $R_{LU}^{(A)}$, Eq.(13), (full line), $R_{LU}^{coh\,(A)}$, Eq.(15), (dashed line) and $R_{LU}^{incoh\,(A)}$, Eq.(16), (dot-dashed line), evaluated at $x_{Bj} = 0.1$ and $0 < t < 0.5$ GeV^2. In **(a)** nuclear effects were taken into account using a longitudinal convolution formula, *i.e.* $X(\zeta)$-rescaling; in **(b)** nucleon off-shell effects were taken into account (see Ref.[17] for more details). In both cases, incoherent scattering dominates the asymmetry for $t \gtrsim 0.05$ GeV^2. An enhancement at $t \approx 0.1$ GeV^2, corresponding to the kinematics of Ref.[11] was found, consistent with the preliminary data.

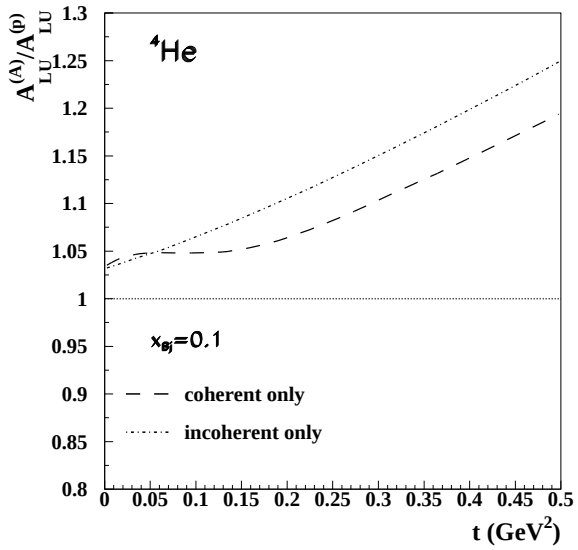

FIG. 3: Ratios $R_{LU}^{(A)}$, Eq.(13), calculated including only coherent scattering terms in both the DVCS and BH contributions to the asymmetry (dashed line), and including only the incoherent terms (dot-dashed line). The nuclear model including off-shell effects was used in the calculations. Notice that the coherent contributions correctly reproduce the off-forward EMC effect calculations of Ref.[17]. Same kinematics as in Fig.2.